Nonlinear Dynamics and Chaos

12

W. Demtröder, *Mechanics and Thermodynamics*, Undergraduate Lecture Notes in Physics, DOI 10.1007/978-3-319-27877-3_12

In Chap. 2 we have discussed the motion of point masses under the influence of forces. The equations of motion are linear differential equations. If the complete initial conditions are given, (e. g. location and velocity at time $t = 0$) the solution of the differential equation determines exactly the future fate of the point mass (its location and velocity at future times $t > 0$), as long as the forces and their changes with time are known.

For cases where the equation of motion has no analytical solutions and requires a numerical integration the accuracy of the results is only limited by numerical uncertainties, which can be minimized by using sufficiently fast computers.

In such cases of exact predictions, the motion of a body or the time development of a system are called *strictly deterministic*. For exact initial conditions, exact predictions of the future development are possible.

If small deviations of the initial conditions cause only small changes of the future development of the system, we call the solutions of the equation of motion stable.

Examples of such stable solutions are the motion of the moon around the earth, or of the earth around the sun. Small perturbation of the central gravitational force field by the influences of the other planets (or in case of the moon by the sun) lead only to small corrections of the trajectories of the earth or the moon, which can be calculated within the framework of perturbation theory. As long as the solutions of the equation of motion are stable, such small corrections do not destroy the predictability of future positions and velocities.

Although we are accustomed in daily life to the normality of stable solutions, there are numerous examples of unstable solutions, where tiny changes of the initial conditions result in a completely different future development of a system, which then lead to completely different final states.

A simple example is a ball, that is released from the point ($x = 0, z = h$) and falls down. During its fall it hits a body with two sloped plain surfaces and a sharp edge at the top (Fig. 12.1). If the initial point is only shifted by a tiny amount δx to the right, the ball hits the right slope of the obstacle and is reflected to the point ($x = x_1, z = 0$) while for $\delta x < 0$ the ball hits the left side and is deflected to the point ($x = -x_1, z = 0$).

A second example is the parametric oscillator (see Sect. 11.7) as an oscillating system that is driven by an external periodic force. It can be realized, for instance, by a simple pendulum with a string length $L = L_0 + \Delta L_0 \cdot \cos(\omega t + \alpha)$ that is periodically changed and a large oscillation amplitude where the restoring force $m \cdot g \cdot \sin\varphi$ can no longer approximated by $m \cdot g \cdot \varphi$ (see Sect. 2.9.6), Eq. 2.79). The equation of motion of such a driven pendulum

$$(L_0 + \Delta L_0 \cos(\omega t + \alpha))\,\ddot{\varphi} + \gamma\dot{\varphi} + g \cdot \sin\varphi = 0 \qquad (12.1)$$

is nonlinear. For certain regimes of the parameters ΔL_0, ω and α (amplitude, frequency and phase of the external force) the amplitude grows until the angel φ exceeds the value π. Then

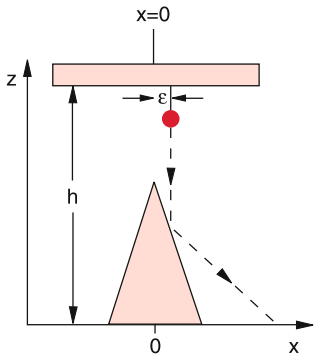

Figure 12.1 The final location of the falling ball depends very sensitive on the initial position around $x = 0$

the periodic pendulum motion changes into an irregular circular motion where the function $\varphi(t)$ shows a chaotic behaviour (Fig. 12.2).

Another example is the motion of a planet that moves in the gravitational field of two stars (double star system) that is quite common in the universe. Its trajectory depends critically on the initial conditions. It can be stable, for instance, but for tiny changes of the initial conditions the motion of the planet becomes unstable. It either leaves the system or it collides with one of the two stars.

A more difficile example is the motion of a body around the planet Saturn in the range of the ring system. Here ranges for the distances r to Saturn are found where the superposition of the gravitational forces by Saturn and by its inner moons leads to unstable trajectories of the body while slightly different radii show stable motions. The unstable ranges are those where the gaps in the ring system occurs. In the unstable ranges the ratio T_b/T_m of the circulation periods of the body and of one of the inner moons equals the ratio p/q of small integers p and q. A very small change of the initial radius r can convert a stable trajectory into an unstable one.

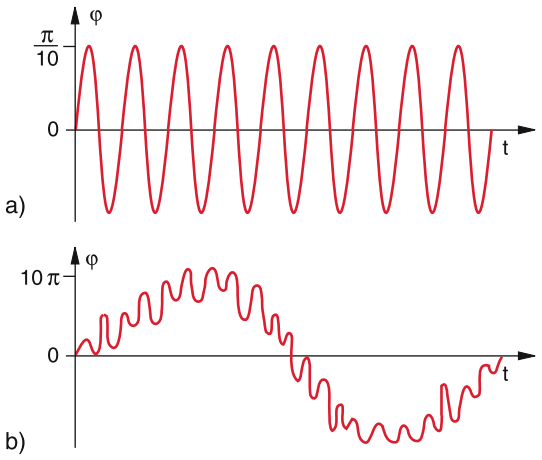

Figure 12.2 Pendulum oscillations driven by an external force. **a** Small amplitude in the stable linear range; **b** in the unstable range with large amplitude. The ordinate scale is in (**b**) 100 times larger than in (**a**)

A similar phenomenon occurs in the asteroid belt between Mars and Jupiter, where the time-dependent gravitational attraction between asteroid and Jupiter leads for certain radii to unstable asteroid trajectories and causes the observed gaps in the asteroid belt.

All of these examples correspond to equations of motion that contain at least one nonlinear term that is responsible for the unstable motion. For the example of the parametric pendulum, these are the nonlinear restoring force $m \cdot g \cdot \sin\varphi$ and the nonlinear driving force. For certain ranges of the parameters a and b (a = ratio of the resonance frequency ω_0 to the driving frequency ω, and b gives the ratio of the amplitudes of driving force to restoring force) the motion becomes unstable.

The solutions of linear equations have the following noteworthy property: They obey the superposition principle, which has been demonstrated in Sect. 11.3 for the example of linear oscillations: If $x_1(t)$ and $x_2(t)$ are solutions of the linear equation, every linear combination $x(t) = a \cdot x_1(t) + b \cdot x_2(t)$ is also a solution.

We will show that this superposition principle no longer holds for the solutions of nonlinear equations It is replaced by another principle: The *scale invariance* or *self-similarity*.

As was illustrated by the forgoing examples, for many parameter ranges there are no stable solutions of nonlinear equations. This means that even for very small changes of the initial conditions the time development of a system leads to completely different final states. Since generally the initial states are not exactly defined (because of measuring uncertainties), the predictability is severely limited for such systems.

Most processes in nature can be described only approximately by linearized equations, although in many cases an admirable accuracy is reached (for example by prediction of moon- or solar eclipses). The exact equation of motion should contain the nonlinear terms. If these terms lead to unstable developments of the system, we called this a **chaotic behaviour**. Examples of such chaotic behaviour can be for instance, found in Meteorology. They demonstrate that the difficulty to predict exactly the forthcoming weather is not an indication of the missing capability of the meteorologists but an inherent feature of the chaotic system.

In spite of these difficulties a lot of surprising statements can be made about the solutions of nonlinear equations and the behaviour of nonlinear systems. The investigation of chaotic systems is the subject of *Chaos Research*, which can be only shortly discussed here. For a more extensive study of this fascinating field the reader is referred to the literature [12.1a–12.6b]

12.1 Stability of Dynamical Systems

A dynamical system changes with time, in contrast to a stationary system, which has reached an equilibrium state that does no longer change in time.

The dynamical system can be described by time-dependent parameters $\xi_i(t)$ ($i = 1, 2, 3, \ldots, N$). The quantities $\xi(t)$ can be, for example, the coordinates $x_i(t)$ and the velocities $v_i(t)$ of a point mass moving on its trajectory, or they characterize the time dependent state of a system of many particles, for instance pressure $p(t)$ and temperature $T(t)$. They can also describe the number of subjects in a biological system where the population changes with time.

If the state of a dynamical system at time t_2 is unambiguously determined by its state at the earlier time $t_1 < t_2$ we call the dynamics deterministic, in contrast to the stochastic or random dynamics, where for the development of the system only probabilities can be given, no certain and unambiguous predictions.

When the state of a system at time t is characterized by the N quantities

$$\boldsymbol{X}(t) = \{\xi_1(t), \xi_2(t), \ldots, \xi_N(t)\} \ , \tag{12.2}$$

which we can condense in the vector $X(t)$, the change of the system in time is described by

$$\dot{\boldsymbol{X}}(t) = \left\{\frac{\mathrm{d}\xi_1(t)}{\mathrm{d}t}, \frac{\mathrm{d}\xi_2(t)}{\mathrm{d}t}, \ldots, \frac{\mathrm{d}\xi_N(t)}{\mathrm{d}t}\right\} \ . \tag{12.3}$$

If the system converges towards a stationary (time-independent) state and reaches it in a finite time t_f the condition

$$\dot{\boldsymbol{X}}(t_\mathrm{f}) = 0$$

must be fulfilled. If the stationary state is only reached at $t = \infty$, the condition is

$$\lim_{t\to\infty} \dot{\boldsymbol{X}}(t) = 0 \ .$$

An example for the first kind is the function

$$X(t) = X_0 + a \cdot t^2 \quad \text{for} \quad t < 0 \quad \text{and} \quad X = X_0 \quad \text{for} \quad t > 0,$$

$$\rightarrow \dot{\boldsymbol{X}}(t) = 2at \quad \text{for} \quad t < 0 \quad \text{and} \quad \dot{X}(t) = 0 \quad \text{for} \quad t \geq 0 \ .$$

In many cases the system approaches a stationary state only asymptotically and reaches it for $t = \infty$.

Example: The population of radioactive atoms, decaying with a decay constant λ is

$$N = N_0 e^{-\lambda t} \ ,$$

it approaches $N(t = \infty) = 0$ only after an infinite time.

Often the situation occurs that the state of a system does not change continuously but in finite steps. An example is the number of living species in a biological population, where the birth rate is not constant over the year but births happen only in spring. Such discrete dynamics can be described by finite difference-equations compared to differential equations for continuous dynamics. For example the number N_{n+1} of subjects in the $(n + 1)$th generation is determined by the population in the nth generation and the birth- and death-rate:

$$N_{n+1} = N_n + B_n - D_n \ , \tag{12.4}$$

where the difference $N_{n+1} - N_n$, which is determined by the birth- and death-rate, is not a continuous but discrete function of time (see Sect. 12.2).

We name the N-dimensional space with the coordinates $\{\xi_1, \xi_2, \ldots, \xi_N\}$ the **phase space** of the system. In this phase space the state of the system at time t_0 is represented by the point $\boldsymbol{X}(t_0)$. The time-development of the system then corresponds to the trajectory $\boldsymbol{X}(t)$ in the phase space. This representation of the time development of the system by a trajectory in the phase space is called the *mapping* of the system. The vector $\dot{\boldsymbol{X}}(t)$, which gives the velocity of the point $\boldsymbol{X}(t)$ in the phase space, maps how fast the system changes its state. The stationary states of the system, given by $\dot{\boldsymbol{X}}(t) = 0$ are called the **fix points**. If the system is deterministic, only one trajectory can pass through each point $X(t)$, which is not a fix point. Only in a fix point many (often an infinite number) of trajectories can concur. Therefore such a fix point is also called an **attractor**. The range of all X-values that converge towards an attractor is called the intake area of the attractor:

In nonlinear systems not only points but also curves or areas can occur as attractors. However, they do not represent fix points (see Example 5).

Examples

1. The undamped harmonic oscillator with linear restoring force $F = -D \cdot x$ has the energy (see Sect. 11.6)

$$E = \frac{m}{2}\dot{x}^2 + \frac{1}{2}Dx^2 \,, \tag{12.5}$$

and the oscillation frequency $\omega_0 = \sqrt{D/m}$.
From (12.5) one obtains immediately the two-dimensional phase space trajectory

$$x^2 + \left(\frac{\dot{x}}{\omega_0}\right)^2 = \frac{2E}{D} \,.$$

In a phase space with the axes x and $\dot{x}/\omega_0$ the trajectory becomes a circle around the origin with the radius $R = \sqrt{2E/D}$ (Fig. 12.3a) For each value of E (initial condition) the system passes with constant frequency a well-defined circle. The motion is stable.

2. For the damped oscillator the energy decreases exponentially (Sect. 11.6). The corresponding trajectory in phase space is obtained from the equation of motion

$$\ddot{x} + 2\gamma\dot{x} + \omega_0^2 x = 0 \,. \tag{12.6}$$

Equation 12.6 can be also written as (see Eq. 11.31)

$$\frac{\mathrm{d}}{\mathrm{d}t}\left(x^2 + \left(\frac{\dot{x}}{\omega_0}\right)^2\right) = -4\gamma\left(\frac{\dot{x}}{\omega_0}\right)^2 \,. \tag{12.7}$$

Equation 12.7 represents in a phase space with coordinates x and $\dot{x}/\omega$ a spiral, which converges against the origin as a stable attractor (Fig. 12.3b)

3. For a negative damping (the energy loss is overcompensated by an external force) the oscillation amplitude increases with time and the trajectory is a spiral with increasing radius, approaching $r = \infty$.

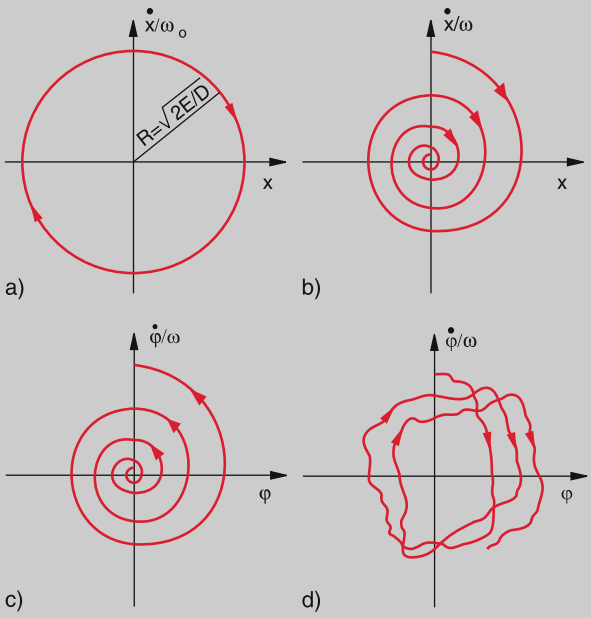

Figure 12.3 Phase space trajectories of the undamped (**a**) and damped (**b**) harmonic ascillators. In (**c**) with negative damping ($\gamma < 0$); (**d**) shows the trajectoriy of the chaotic motion in the unstable range of the nonlinear forced oscillator with large amplitude

For a pendulum with negative damping, the deflection angle φ and its time derivative $\mathrm{d}\varphi/\mathrm{d}t$ can be used as coordinates in phase space. One then obtains the open spiral in Fig. 12.3c.

4. For the parametric oscillator with the equation of motion (12.1) the trajectory in phase space that corresponds to the motion in the chaotic range, is an irregular non-closed curve, which is schematically shown in Fig. 12.3d.
5. A rotating paraboloid $z(r) = a \cdot r^2 = a \cdot (x^2 + y^2)$ contains steel balls that participate in the rotation (Fig. 12.4). The forces that act on the balls are the gravity $m \cdot g$, the centrifugal force $m\omega^2 \cdot r \cdot \hat{\boldsymbol{r}}_0$ and a friction force $F_\mathrm{f} \propto v_\parallel$ parallel to the wall. A stable path for the balls is at the heights $z = z_s = (1/2)(\omega^2/g)r^2$ where the vector sum of gravity force and centrifugal force is perpendicular to the wall (Fig. 6.19b).

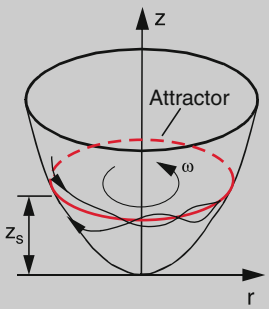

Figure 12.4 Potential surface and attractor curve (*red*) for the example 5

Balls at $z > z_s$ experience a force parallel to the wall, that drives the balls downwards, balls with $z < z_s$ are driven upwards. For a given frequency ω the curve $z = a \cdot r_s^2$ as stable curve is an attractor for all unstable circular trajectories.

6. A further interesting example is the simple pendulum (Eq. 2.79a) with the equation of motion

$$m \cdot L \cdot \ddot{\varphi} + m \cdot g \cdot \sin\varphi = 0 \,. \tag{12.8}$$

Integration and division by $m \cdot L$ gives with $\omega^2 = g/L$

$$\tfrac{1}{2} \cdot \dot{\varphi}^2 - \omega^2 \cdot \cos\varphi = C \,. \tag{12.9}$$

Plotting the trajectories in a phase diagram one obtains, depending on the values of φ the curves in Fig. 12.5. They are closed for $\varphi < \pi$ but lead into an unstable region for $\varphi \geq \pi$, here the angle increases continuously. The two regions are separated by the red curve, which is called the *seperatrix*. Multiplying (12.9) with $m \cdot L^2$ and adding $m \cdot g \cdot L$ to both sides yields

$$\begin{aligned} &\tfrac{1}{2} m \cdot L^2 \dot{\varphi}^2 + m \cdot L g (1 - \cos\varphi) = C_1 \\ &\text{with } C_1 = C \cdot mL^2 + mgL \\ &\Rightarrow E_{\text{kin}} + E_{\text{pot}} = C_1 = E \,. \end{aligned} \tag{12.10}$$

This shows that the seperatrix is the curve on which $E = 0 \rightarrow C = -g/L$. The point A in Fig. 12.5 is the attractor, its intake area are all φ-values with $|\varphi| < \pi$. The point B is a metastable equilibrium point, because it corresponds to the metastable position of the pendulum with $\varphi = \pi$. Every small perturbation can completely change the state.

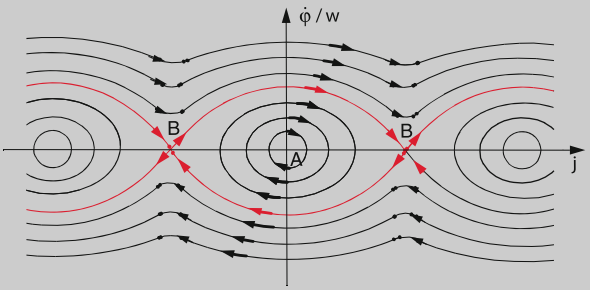

Figure 12.5 Phase space trajectories of the non-linear undamped oscillator. The *red curve* is the seperatrix between the stable ($|\varphi| < \pi$) and unstable ($|\varphi| > \pi$) range ◀

We will now define more quantitatively the stability of fix points of a dynamical system. We consider at first a nonlinear system that depends only on one coordinate x. At discrete times t_n it passes through the coordinates x_n. The value x_{n+1}, which the system takes at the time t_{n+1} depends on the foregoing value x_n:

$$x_{n+1} = f(x_n) \,, \tag{12.11}$$

where the function f describes the development of the system.

If the system has reached a fixpoint, the development stops and stays stationary. This means

$$x_\text{f} = f(x_\text{f}) \,. \tag{12.12}$$

If the system converges towards a fixpoint ($x_\text{f} = \lim_{n\to\infty}(x_n)$) the deviation

$$\delta = x_n - x_\text{f} \rightarrow 0$$

must converge towards zero for $n \rightarrow \infty$. For the difference δ_{n+1} one obtains

$$\begin{aligned} \delta_{n+1} &= x_{n+1} - x_\text{f} = f(x_n) - x_\text{f} \\ &= f(x_\text{f} + \delta_n) - x_\text{f} \,. \end{aligned} \tag{12.13}$$

Expanding $f(x_\text{f} + \delta_n)$ into a Taylor series around x_f and neglecting for small δ_n the higher order terms, Eq. 12.13 gives

$$\delta_{n+1} = \left.\frac{\mathrm{d}f(x)}{\mathrm{d}x}\right|_{x=x_\text{f}} \cdot \delta_n \,. \tag{12.14}$$

If the deviations δ_n should converge towards zero for $n \rightarrow \infty$ the condition

$$\left|\left.\frac{\mathrm{d}f(x)}{\mathrm{d}x}\right|_{x=x_\text{f}}\right| < 1 \tag{12.15}$$

must be fulfilled.

A system that starts with two slightly different initial values x_0 and $x_0 + \varepsilon_0$ can only reach the same final stationary state (fixpoint), if condition (12.15) hold.

The deviation after the first step is according to (12.11)

$$x_1 + \varepsilon_1 = f(x_0 + \varepsilon_0) \Rightarrow \varepsilon_1 = f(x_0 + \varepsilon_0) - f(x_0) \,,$$

and after the second step

$$x_2 + \varepsilon_2 = f(x_1 + \varepsilon_1) = f(f(x_0 + \varepsilon_0)) = f^2(x_0 + \varepsilon_0) \,,$$

and therefore after the nth step

$$\varepsilon_n = f^n(x_0 + \varepsilon_0) - f^n(x_0) \,. \tag{12.16}$$

As a measure of the stability, one defines the *Ljapunov exponent* λ

$$\begin{aligned} \lambda(x_0) &= \lim_{n\to\infty} \lim_{\varepsilon_0 \to 0} \frac{1}{n} \log \left| \frac{f^n(x_0 + \varepsilon_0) - f^n(x_0)}{\delta_0} \right| \\ &= \lim_{n\to\infty} \frac{1}{n} \log \left| \left. \frac{\mathrm{d}f^n(x)}{\mathrm{d}x} \right|_{x=x_0} \right| \,. \end{aligned} \tag{12.17}$$

The condition (12.15) can then be written for large values of n as

$$\delta_{n+1} = \delta_n \cdot e^\lambda \,. \tag{12.18}$$

For $\lambda < 0$ the system converges against a stable fixpoint. For $\lambda > 0$ the deviations increase exponentially and no fixpoint exists (Fig. 12.6). The case $L = 0$ will be discussed later.

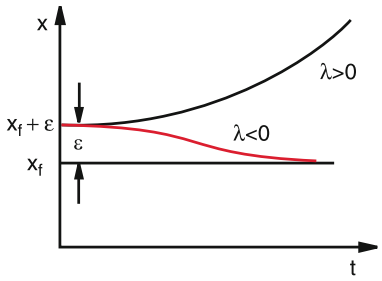

Figure 12.6 Time development of a small deviation ε from the fixpoint x_f for $\lambda > 0$ and $\lambda < 0$

The stability of fixpoints is illustrated by Fig. 12.7a, where the schematically drawn trajectory in the phase space $(x, \dot{x})$ is the representation of a one-dimensional equation of motion. The intersection points of the curve with the horizontal line $\dot{x} = 0$ are the fixpoints. The points x_1 and x_3 are unstable fixpoints, because small negative deviations bring the system to negative velocities, that further remove the system from the fixpoint, while positive deviations cause positive velocities that bring the system further upwards in the diagram. On the other hand is x_2 a stable fixpoint because any deviation brings the system back to x_2. It acts as attractor with a intake range from x_1 to x_3. All states of the system within this range tend to converge to x_2.

An example for such a system is a particle with mass m in a double well potential (Fig. 12.7b) with the potential energy

$$E_{\text{pot}}(x) = -ax^2 + bx^4 \,, \tag{12.19}$$

where the nonlinear force

$$F_x(x) = -\frac{\mathrm{d}E_{\text{pot}}}{\mathrm{d}x} = 2ax - 4bx^3 \tag{12.20}$$

acts on the particle. Its equation of motion is

$$m\ddot{x} - 2ax + 4bx^3 = 0 \,. \tag{12.21}$$

Energy conservation $(1/2)\, m\dot{x}^2 + E_{\text{pot}}(x) = E$ yields the velocity of the particle

$$v = \dot{x} = \sqrt{\frac{2}{m}\left(E - E_{\text{pot}}\right)} \,. \tag{12.22}$$

For $E = E_{\text{pot}} \to E_{\text{kin}} = 0$ the velocity becomes $\dot{x} = 0$ at the position $x = 0$ because there is $E_{\text{pot}}(0) = 0$. However, this is no stable fixpoint, because small deviations bring the particle either to the left or the right minimum. If its velocity converges to zero due to frictional losses, it finally rests in one of the two minima at $x = \pm\sqrt{a/2b}$. They are stable fixpoints. The intake range for the fixpoint $x_1 = \sqrt{a/2b}$ includes all x-values $x > 0$, while for the other fixpoint $x_2 = -\sqrt{a/2b}$ all negative x-values $x < 0$ belong to its intake range.

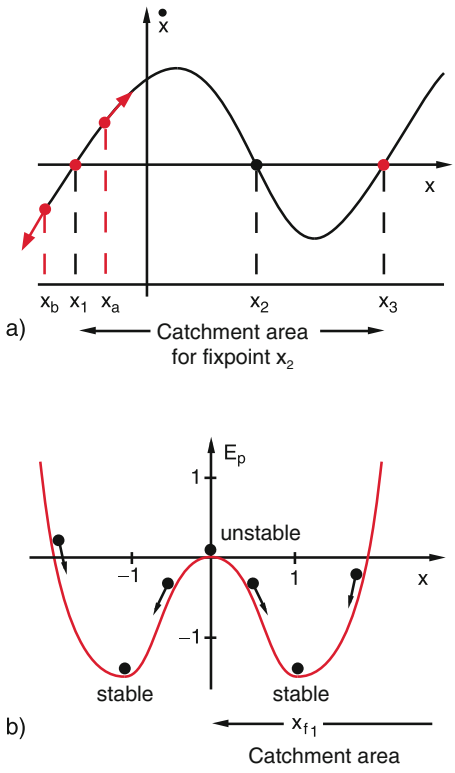

Figure 12.7 **a** Trajectory in phase space with unstable fixpoints x_1, x_3 and an attractor at x_2 with a catchment area from x_1 to x_3. **b** Particle in a potential $E_{\text{pot}} = -ax^2 + bx^4$ (for $a = 2$, $b = 0.5$) has a maximum at $x = 0$, which is unstable and a stable minimum, where $\dot{x} \to 0$

12.2 Logistic Growth Law; Feigenbaum-Diagram

A very instructive example of a nonlinear system is the biological population where the number N_{n+1} of the members in the $(n + 1)$th generation is proportional to the number N_n in the foregoing generation.

$$N_{n+1} = a \cdot N_n \,, \tag{12.23}$$

where a is the growth factor. Due to food shortage the growth factor a decreases to $a(1 - b \cdot N_n)$, because the food consumption is proportional to the number N_n of consumers. Inserting this into (12.23) gives

$$N_{n+1} = a \cdot N_n(1 - bN_n) \,. \tag{12.24}$$

A stationary state (fixpoint) is reached for

$$N_{n+1} = N_n = N_{\text{st}} \Rightarrow b = \frac{a-1}{a \cdot N_{\text{st}}} \,. \tag{12.25}$$

This is realized for $a = 1 \Rightarrow b = 0$. No food shortage is present.

For $a < 1$ is $N_{n+1} < N_n$ i. e. the population decreases even for $b = 0$ when no food shortage occurs, while for $a > 1$ the

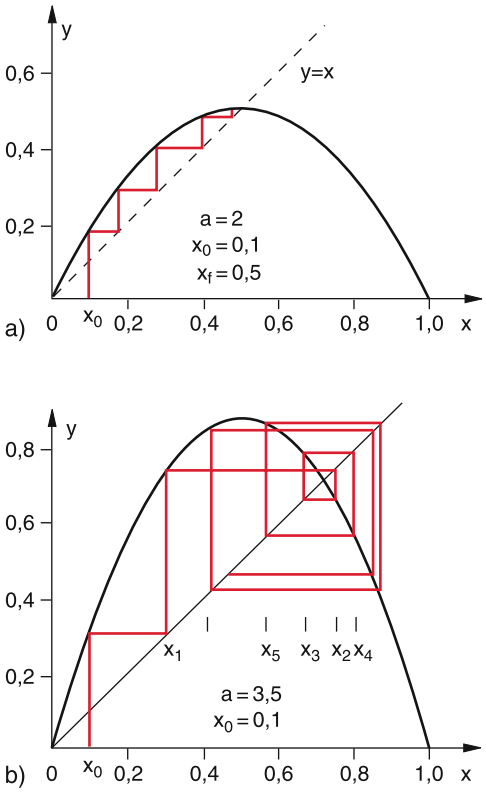

Figure 12.8 Logistic diagram: **a** in the stable range $a = 2$ with stable fixpoint $x_f = 0.5$; **b** in the oscillation range with $a = 3.5$

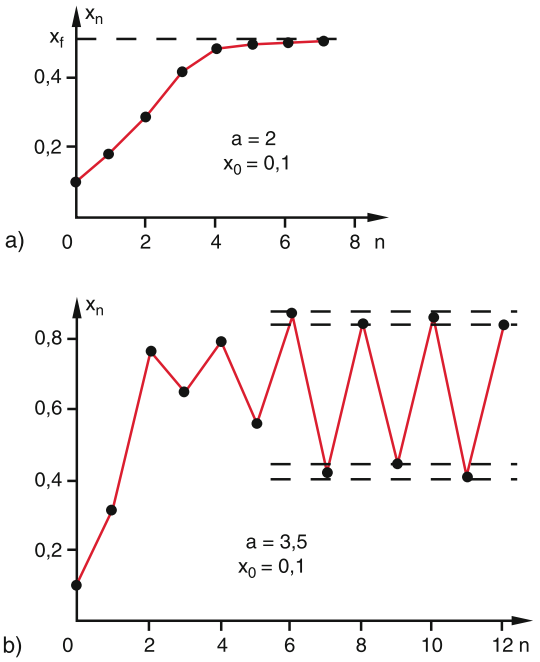

Figure 12.9 The first members of the series x_n: **a** fast convergence for $a = 2$; **b** oscillating behaviour for $a = 3.5$

population increases until the food shortage $b \cdot N_n$ increases and brings the effective growth factor again back to 1.

With the normalization $x = bN \leq 1$ (12.24) converts to the **Verhulst-Equation**

$$x_{n+1} = ax_n(1 - x_n) = ax_n - ax_n^2 \,. \qquad (12.26)$$

With the given normalization $x \leq 1$ the possible values of the parameter a are restricted to the interval $0 \leq a \leq 4$.

The solution of Eq. 12.26 for the different generations n and their dependence on the growth parameter a can be illustrated graphically, when the parabola $y = ax - ax^2$ and the linear slope $y = x$ are plotted in a (y, x)-diagram (Fig. 12.8). For each value $x_n < 1$ one finds from (12.26) the corresponding value x_{n+1} as ordinate $y = ax - ax^2 = x_{n+1}$ on the parabola. In order to find the new starting point x_{n+1} one must go from $(x_n, y_n = x_{n+1})$ into the horizontal direction to the intersection with the straight line $y = x$. A vertical line through this intersection point reaches the parabola at the point $(x_{n+1}, y_{n+1} = x_{n+2})$.

In this way one obtains the sequence x_n $(n = 0, 1, 2, \ldots)$ as step function starting from an arbitrarily chosen initial starting point x_0.

This is illustrated in Figs. 12.8a and 12.9a for $x = 0.1$ and $a = 2$. One can see that the sequence x_n converges relatively fast against the fixpoint $x_f = 0.5$.

A completely different situation occurs for the same starting point $x_0 = 0.1$ but another growth factor $a = 3.5$ (Figs. 12.8b and 12.9b). Here the sequence oscillates between 4 limiting values.

It turns out that for $a > 3.57$ the behaviour of the sequence depends critically on the growth factor a, while the values of the sequence memers x_n do not depend on the initial value x_0 as long as $a < 3.57$.

Plotting the limits $\lim_{n\to\infty} x_n$ of the logistic equation (12.26) as a function of the growth parameter a one gets the Feigenbaum-diagram shown in Fig. 12.10, which was first published 1978 by *S. Großmann* [12.6a] and analysed by ***M. Feigenbaum*** [12.6b]. One can see the following surprising results of the logistic growth law:

- For $a \leq 1$ the sequence x_n converges against zero. The closer the value of a comes to $a = 1$ the slower the sequences converges. The stable fixpoint is $x_f = 0$.
- For $1 < a < 3$ a stable fixpoint exists: $\lim_{n\to\infty} x_n = x_f < 1$ but $\neq 0$.
- For $3 < a_\infty$ the values of x_n oscillate between 2^k limiting values, where $a_\infty = 3.57$ (see below). The exponent k is $k = 1$ for $3 < a < 3.449$; $k = 2$ for $3.449 < a < 3.544$. The points (a, x) in the Feigenbaum diagram where k increases by 1 are called **bifurcation points**. At the first bifurcation point in Fig. 12.10 the curve $x_f = 1 - 1/a$ represents the fixpoints x_f as a function of a, until $a = 3$, where the curve $x_f(a)$ splits into two curves. These cures give the limits $x_f(a)$ as a function of the growth parameter a between which the values of x_n oscillate. Each of these curves splits again at the second bifurcation point, etc.

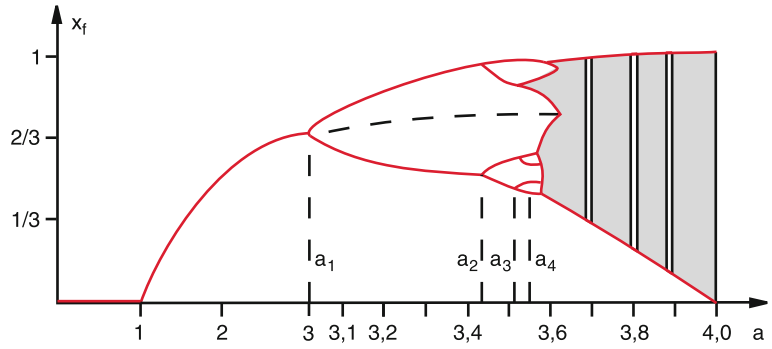

Figure 12.10 Feigenbaum diagram: Value of the fixpoint x_f as a function of the control parameter a. The values a_i give the bifurcation points $a_1 = 3.0$; $a_2 = 3.449\ldots$; $a_3 = 3.544\ldots$; $a_4 = 3.564\ldots$

The system has therefore 2^k attractors for all values of the growth parameter a in the range $a_k \le a \le a_{k+1}$ between the bifurcation points a_k and a_{k+1}.
With increasing values of a the interval between two bifurcation points becomes smaller and smaller. The values of the bifurcation points of order k follow a geometrical sequence

$$a_k = a_\infty - c \cdot \delta^{-k} \quad \text{for} \quad k \gg 1 \,. \tag{12.27}$$

For the distance $\Delta_k = a_k - a_{k-1}$ we obtain

$$\Delta_k = c \cdot \delta^{-k}(\delta - 1) \,. \tag{12.28}$$

The Feigenbaum-constant $\delta_F = \lim_{n\to\infty}(\Delta_k/\Delta_{k+1})$ has the numerical value

$$\delta_F \approx 4.669201660910\ldots \,.$$

The sequence of bifurcation points converges against the limit

$$a_\infty = \lim_{k\to\infty} a_k = 3.5699456\ldots \,.$$

The Ljapunov exponent λ is in the range $3 < a < a_\infty$ always negative, except at the bifurcation points where is $\lambda = 0$.

- In the range $a_\infty < a < 4$ chaotic regions occur where the values of the fixpoints scatter randomly. Here is the Ljapunov exponent $\lambda > 0$ (Fig. 12.11) between these chaotic ranges periodic windows appear where stable fixpoints occur. The sequence x_n oscillates between these fixpoints. The Ljapunov exponent λ is negative in these windows. With increasing values of the growth parameter a the chaotic regions more and more displace the windows of stable regions.
- In the chaotic regions rational start values give fixpoints, while for irrational start values no convergence is possible For $a = 4$ the logistic equation

$$x_{n+1} = 4x_n(1 - x_n) \tag{12.29}$$

can be exactly solved and gives the solution

$$x_n = \sin^2(2^n \pi x_0) \,, \tag{12.30}$$

where x_0 is the start value.

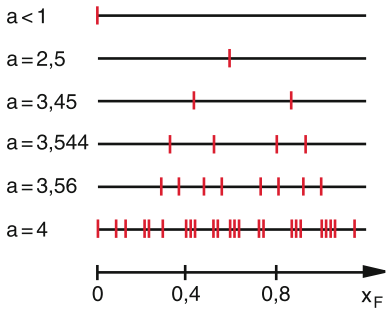

Figure 12.11 The fixpoints of the logistic mapping for different values of the parameter a for illustration of the bifurcation

12.3 Parametric Oscillator

The equation of the undamped parametric oscillator, depicted in Fig. 11.25 with the pendulum length

$$L(t) = L_0 - \Delta L_0 \cos \Omega t \tag{12.31}$$

and $\Delta L_0/L_0 \ll 1$, can be written as

$$\ddot{\varphi} + \omega_0^2 \left[1 + \frac{\Delta L_0}{L_0} \cos \Omega t\right] \sin\varphi = 0 \,, \tag{12.32}$$

where the approximations

$$\frac{1}{L} = \frac{1}{L_0\left(1 - \frac{\Delta L_0}{L_0}\cos\Omega t\right)} \approx \frac{1}{L_0}\left(1 + \frac{\Delta L_0}{L_0}\cos\Omega t\right)$$

have been used with the frequency

$$\omega^2 = \omega_0^2 \left[1 + \frac{\Delta L_0}{L_0} \cos \Omega t\right] \,.$$

Introducing the abbreviations $\omega_0^2 = g/L_0$; $\alpha = \omega_0^2/\Omega^2$; $\beta = \Delta L_0/L_0$ and $\tau = \Omega \cdot t$ the Eq. 12.32 converts into the Mathieu-equation

$$\varphi'' + \alpha\,(1 + \beta\cos\tau)\,\varphi = 0 \,, \tag{12.33}$$

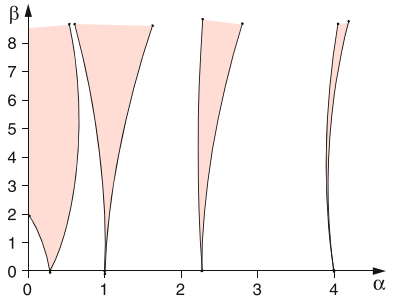

Figure 12.12 Stable (*white*) and unstable (*red*) ranges for the solutions of the Mathieu equation

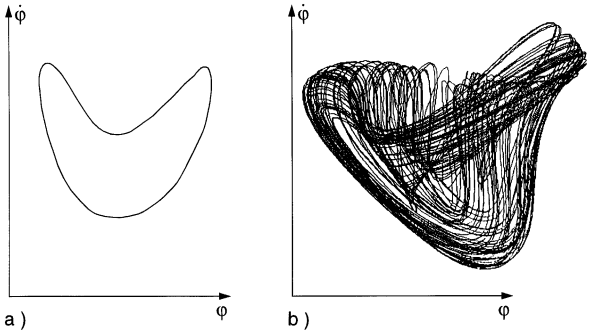

Figure 12.14 Phase diagram of the parametrically driven pendulum **a** in the stable, **b** in the unstable region

where $\varphi'' = \mathrm{d}^2\varphi/\mathrm{d}\tau^2$. The solutions of this linear differential equation depend on the parameters α and β. There exist stable solutions for certain ranges (α, β) which are shown as white areas in Fig. 12.12 while for the red areas (resonance ranges) unstable solutions exist, where φ increases unlimited.

The first instable range appears for $\alpha = (1/4), \rightarrow \Omega = 2\omega_0$. This is the parameter range which a child instinctively uses to enhance the oscillation amplitude of its swing by uplifting and lowering its centre of mass at the right moment twice per oscillation period. Without damping the oscillation amplitude becomes infinite in the red regions and the solutions of (12.33) lead to useless results.

The situation changes if we do not use the approximate linear equation but the exact nonlinear equation (12.32) for the solution of the problem. We start with the trivial case $\varphi = 0$, where the pendulum does not perform angular oscillations $\varphi(t)$ but only vertical periodic changes of the pendulum length $L(t)$. The mass m then executes vertical oscillations with the exciting frequency Ω, where always $\varphi = 0$. This is true for $\alpha < 1/4$ and $\beta \ll 1$. If for $\alpha = 1/4$ the amplitude exceeds a critical amplitude β_c the oscillation becomes unstable and the vertical motion switches into a φ-oscillation (Fig. 12.13) with an amplitude that depends on the parameter β. The frequency ω_0 of this $\varphi(t)$ oscillation is one half of the exciting frequency Ω $(\omega_0 = (1/2)\,\Omega)$. At the bifurcation point B in Fig. 12.13 a doubling of the period length T occurs. When further increasing β, more and more bifurcation points are passed until the chaotic range is reached where the motion of the pendulum becomes random. Here a statistic motion of vertical and angular oscillation takes place. The phase diagram of the regula and chaotic ranges is shown in Fig. 12.14.

In the chaotic regime the motion is very sensitive to small changes of the initial conditions. Plotting $\varphi(t)$ against t small changes of $\varphi(0)$ or $\mathrm{d}\varphi/\mathrm{d}t(0)$ result in large changes of $\Delta\varphi(t)$ which can grow exponentially with time t [12.4].

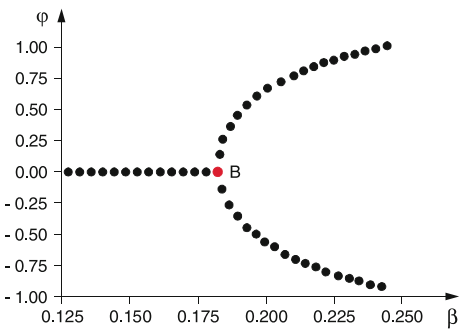

Figure 12.13 The first bifurcation of the pendulum that oscillates initially only vertical. The abscissa $\beta = \Delta L/L_0$ corresponds in the stability diagram of Fig. 12.12 a vertical line

12.4 Population Explosion

We will describe the growth of the world population by a simple model that allows in spite of its simplicity, a good insight into the problem [12.5].

We will take $z_f(t)$ as the female and $z_m(t)$ as the male population at time t. We denote the death rate of the females as $a_f \cdot z_f$ and that of the males as $a_m \cdot z_m$. The birth-rate is proportional to the product $z_f \cdot z_m$. For the change of the population per unit time we then obtain

$$\dot{z}_m = -a_m z_m + b_m z_m z_f \,, \tag{12.34a}$$

$$\dot{z}_f = -a_f z_f + b_f z_f z_m \,. \tag{12.34b}$$

The "symbiosis"-terms $b_m z_m \cdot z_f$ and $b_f \cdot z_f \cdot z_m$ cause the nonlinearity of the equation and couple them with each other.

It turns out that birth rates and death rates do not differ much between males and females. We therefore can approximate $a_m = a_f = a$ and $b_m = b_f = b$. Furthermore the population statistics shows that the populations of males and females is approximately equal, i. e. $z_m \approx z_f$.

With these assumptions we obtain for the total population $z = z_m + z_f$ by addition of the two Eqs. 12.34a,b the nonlinear equation

$$\dot{z} = -a \cdot z + \frac{b}{2} z^2 \,. \tag{12.35}$$

For $b = 0$ (zero birth-rate) we get the solution

$$z(t) = z_0 \mathrm{e}^{-at} \,. \tag{12.36}$$

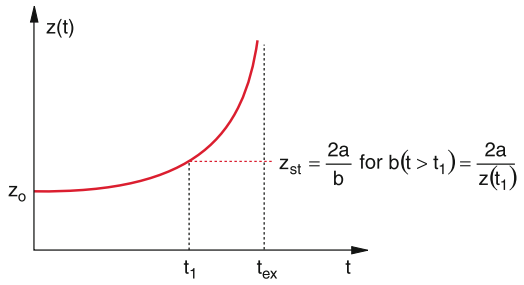

Figure 12.15 Population explosion for fixed values of a and b (*red curve*). If the birth rate b is suddenly reduced to $b = 2a/z(t_1)$ at the time t_1 the population stagnates at $z = z(t_1)$ (*red dashed lines*)

For $a = 0$ and $b \neq 0$ (zero death rate) one obtains an unlimited growth

$$z(t) = z_0 \frac{2}{2 - bz_0 t} , \tag{12.37}$$

as can be verified by inserting (12.37) into(12.36). After a time

$$t_{ex} = \frac{2}{bz_0} , \tag{12.38}$$

the population grows to infinity with our unrealistic assumption $a = 0$.

For $a \neq 0$ and $b \neq 0$ the solution of (12.36) is

$$z(t) = z_0 \frac{2a}{bz_0 - 2 \cdot (bz_0/2 - a)\, e^{+at}} . \tag{12.39}$$

For $a = bz_0/2$ birth rate and death rate just compensate and the population remains stable ($dz/dt = 0$) at its initial value z_0 (Fig. 12.15). **Note**, that the birth-rate depends quadratic on the population, but the death rate only linearly.

For $bz_0 > 2a$ is $dz/dt > 0$ and the population "explodes", At the finite time

$$t = t_{ex} = -\frac{1}{a} \ln \left(1 - \frac{2a}{bz_0}\right) \tag{12.40}$$

the population becomes $z(t_{ex}) = \infty$. **Note**, that in our model this explosion takes place not at $t = \infty$ but at the finite time t_{ex}. Of course, in reality the death rate would increase and the birth rate decrease *before* this time, because of food shortage and conflicts and wars for food supply. In order to avoid such catastrophic situations, the condition $a \leq b \cdot z_{st}/2$ must be reached early enough. Since in our real world the death rate decreases (in particular for children), due to a better medical treatment and a larger food supply, the birth rate $b \cdot z2/2$ has to be drastically reduced in order to avoid this catastrophic case. Comparing in Fig. 12.16 the growth function (12.39) of our model with the real population growth as investigated by the UNESCO, one can see that the population growth proceeds with increasing growth factor $(b \cdot z_0/2 - a)$. While within the time span from 1750 to 1880 the doubling time of the population was 130 years, it dropped from 1950 to 1985 to 35 years! Therefore the actual population curve $z(t)$ increases faster than the growth function (12.39) of our model. This aggravates the problem further.

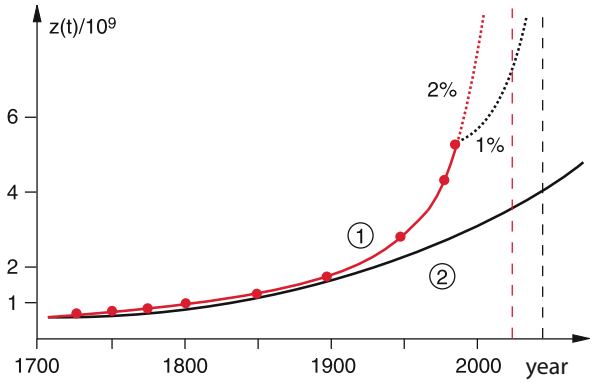

Figure 12.16 Comparison of the population development, empirically determined by the UNO (*curve 1*) with the model of Eq. 12.18 for the numerical values $bz_0/2 - a = 0.003$ for the year 1750 (*curve 2*). The *dashed red curve* is the extrapolation assuming a net growth of 2%. The *black dashed curve* for 1%

Example

For the year 1992 the world population was estimated as $z = 6 \cdot 10^9$. With an average life expectation $\tau = 50$ years the death rate constant becomes $a = 1/\tau = 0.02$ and the death rate $a \cdot z = 120$ Million/year. With an average birth rate of 240 Millions/year the population increases by 2% per year, which means by 120 Millions. Under the assumption of constant birth and death rates the population would double after 50 years. With an increasing growth factor, which is in reality observed, the doubling time would be shorter.

In fact, the real growth factor increases with time.

Inserting the numerical values into (12.40) gives the "explosion time" when the population becomes infinite:

$$t_{ex} = -50 \cdot \ln \frac{0.02}{0.04} = 50 \ln 2 \approx 35 \text{ years} .$$

This means that without decreasing the birth rate the catastrophe will happen in 35 years, which means in the year 2050.

Even when the birth rate is lowered to such a value, that the net population growth decreases to 1%, t_{ex} increases only to 55 years, which means that the catastrophe is not abandoned but only delayed. ◀

12.5 Systems with Delayed Feedback

In many real situations, systems with delayed feedback are found. An example is a microphone that receives not only the direct words of the speaker, but also, with a time delay, the output

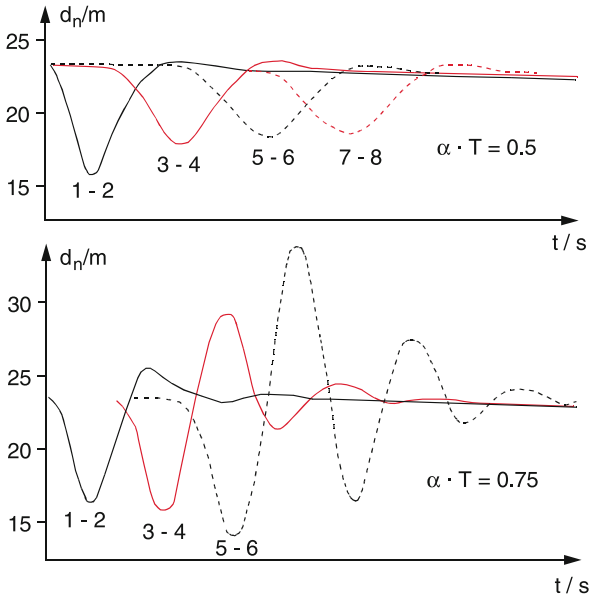

Figure 12.17 Time variation of the distance $d_n = x_n - x_{n+1}$ in a car convoy, when the first car ($n = 1$) brakes and accelerates again, for two different values of $a \cdot T$ [12.7]

of a loud speaker in a large room that amplifies this speech. This time-delayed signal received by the microphone, is again fed into the amplifier and the loud speaker. If the electronic system is not optimized to handle this problem properly, an overload of the loud speaker occurs, resulting in a distortion of the words or even to loud howling noise.

Another example that is a nuisance for every motorist, is the traffic jam arising without obvious reasons when the traffic density surpasses a critical value. We will discuss the reasons for this situation.

In a car sequence on the motorway the driver of the $(n + 1)$ car changes his speed v_{n+1}, if the foregoing nth car diminishes his sped v_n. The more n brakes the more $(n+1)$ does so. because of the finite reaction time T the change of his velocity occurs with a time delay T. We therefore assume, that the braking (deceleration) of $(n + 1)$ at time $t + T$ is proportional to the velocity difference $v_n(t) - v_{n+1}(t)$.

$$\ddot{x}_{n+1}\,(t + T) = a \cdot [\dot{x}_n(t) - \dot{x}_{n+1}(t)] \ . \tag{12.41}$$

The factor a states how strongly the driver $(n + 1)$ reacts on the change of the relative velocity $v_n(t) - v_{n+1}(t)$. It can depend on his velocity v_{n+1}, on the distance $d_n(t) = x_n - x_{n+1}$ and on the reaction time T.

The most simple case is present for $a =$ constant. Even for this case (12.41) cannot be solved analytically, but only numerical solutions exist. They are plotted in Fig. 12.17 for an initial distance $d(t = 0) = 23\,\text{m}$ and for different values of the product $a \cdot T$.

The curves $d_n(t)$ illustrate, that for $a \cdot T = 0.5$ the distance changes decrease for increasing n. This means, when the first driver brakes, a damped distance wave propagates along the following cars. For the 10th driver it is barely noticeable. For the higher value $a \cdot T = 0.75$, however, the distance changes increase with n. If the minimum of the distance wave reaches $d = 0$ the two sequenced cars collide and cause a traffic jam.

But also without collision a jam can arise.

When driver n brakes because the foregoing car reduces its speed, he will generally over-react and reduces his speed below that of the foregoing car. The following car $(n + 1)$ reduces its speed even more, until the $(n + x)$th car comes to a standstill. Such a traffic jam often occurs when the traffic density is high and the distance between the cars is small.

In order to avoid such unnecessary jams the product $a \cdot T$ ust be sufficiently small. Since the reaction time of most drivers has a lower limit of about 0.1 s (at a speed of 130 km/h this time corresponds to a distance of 36 m) **the best way for safe driving without causing a traffic jam is a sufficiently large distance between successive cars**.

12.6 Self-Similarity

The linear differential equation

$$\dot{x} = -a \cdot x(t) \tag{12.42}$$

has the solution

$$x(t) = x_0 \cdot \mathrm{e}^{-at} \ . \tag{12.43}$$

The arbitrary initial value of x and the constant parameter a determine the time dependence of $x(t)$. If we choose two solutions $x_1(t)$ and $x_2(t)$ with different initial conditions, e. g. with different values of $x_1(0)$ and $x_2(0)$ every linear combination $c_1 \cdot x_1(t) + c_2 \cdot x_2(t)$ is again a solution of (12.42), and is again an exponential function.

For a nonlinear equation this is no longer true, as can be exemplified by the equation

$$\dot{x} = -a \cdot x^2 \ . \tag{12.44}$$

The solution of this nonlinear equation is

$$x(t) = \frac{x_0}{1 + ax_0 t} \ . \tag{12.45}$$

For two different solutions

$$x_1(t) = \frac{x_{01}}{1 + ax_{01}t} \quad \text{and} \quad x_2(t) = \frac{x_{02}}{1 + ax_{02}t} \ ,$$

the sum $x_1(t) + x_2(t)$ is not a solution of (12.44).

For long times t, when $a \cdot x_0 \cdot t \gg 1$ the function $x(t)$ can be approximated by

$$x(t) \approx \frac{1}{at} \ . \tag{12.46}$$

Now the solution does not depend on the initial value x_0.

When the time is measured in other units (for example in hours instead of seconds) the time t is replaced by $\lambda \cdot t$. This converts (12.46) to

$$x(\lambda \cdot t) = \frac{1}{\lambda a t} = \frac{x(t)}{\lambda} \; . \tag{12.47}$$

The solutions are similar even for different time scales! For example, with $\lambda = 10$ one obtains the same time behaviour for the function $x(\lambda t)$ as for $x(t)$ if a tenfold stretched time scale is used.

This scale similarity can be mathematically expressed as

$$x(\lambda t) = \lambda^{\kappa} \cdot x(t) \; . \tag{12.48}$$

The quantity κ is the scale exponent or similarity exponent. For the nonlinear equation (12.44) with the approximation (12.46) is $\kappa = -1$.

The time dependence of the solution $x(t)$ of (12.48) can be expressed as

$$x(t) \propto t^{\kappa} \; , \tag{12.49}$$

because this gives $x(\lambda t) \propto \lambda^{\kappa} \cdot x(t)$.

Note: For linear equations such a scale similarity does not exist. This can be seen by replacing in (12.43) t by $t' = \lambda t$. This gives another exponential decay

$$x(t') = x_0 \cdot \mathrm{e}^{-a\lambda t} = \frac{(x(t))^{\lambda}}{x_0^{\lambda - 1}} \; . \tag{12.50}$$

Only if the relaxation constant a is changed to a/λ the same time behaviour is obtained.

This means: The constant "a" fixes a time scale for the solution of the linear equation (12.42) After the time $t = 1/a$ has $x(t)$ decreased to $1/\mathrm{e}$ of its initial value at time $t = 0$. The mean lifetime $\tau = 1/a$ gives a natural time scale for the solution (12.43).

In contrast to this behaviour of the solutions of linear equations the parameter a in the nonlinear equation does not determine such a benchmark. An arbitrary time stretch can be always compensated by a corresponding change of the x-scale.

> The self-similar solutions of nonlinear equations do not have a natural benchmark.

This is not only valid for time-dependent problems but also for many other interesting phenomena, which can be only partly presented in the next section. For further examples the reader is referred to the literature [12.1a–12.6b].

12.7 Fractals

The measured length of a real coastline with many bays, juts and mountain ledges depends on the resolution of the measuring gauge. This is illustrated by the famous example of

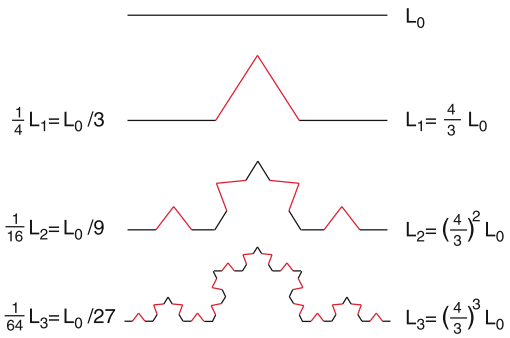

Figure 12.18 Construction of Koch's curve

the *Koch's curve* that is constructed in the following way: A straight line with length L_0 is divided into three sections. The middle section is replaced by the two sides of an equilateral triangle (second line in Fig. 12.18). Each section has the length $L_0/3$, the total length is then $(4/3)\,L_0 = 1.33L_0$. Now each of the 4 sections is again divided into three subsections and the middle subsection is replaced by the two sides of an equilateral triangle (third line in Fig. 12.18). The total length is now $L = (16/9)\,L_0 = (4/3)^2 L_0 = 1.78L_0$.

This procedure is continued. After n steps the total length is

$$L_n = \left(\frac{4}{3}\right)^n L_0 \; . \tag{12.51}$$

With increasing number n of steps, the total length L_n becomes infinite.

$$\lim_{n \to \infty} L_n = \infty$$

The Koch's curve shows self-similarity, because at the nth iteration the scale length l_n (i. e. the length l_n of each subsection) is $l_n = L_0/3^n$. The total number of subsections is $N_n = 4^n$. We therefore obtain the relation

$$N(l/3) = 4N(l) \; , \tag{12.52}$$

because at each step the scale length is reduced by a factor 3, but the number of subsections increases by the factor 4. The comparison with the scale law (12.49), which can be written as

$$N(\lambda \cdot l) = \lambda^{\kappa} \cdot N(l) \tag{12.53}$$

yields the value $\lambda = 1/3$ and $\lambda^{\kappa} = 4$. The scale parameter κ is then

$$\kappa = -\frac{\ln 4}{\ln 3} = -1.2618 \; .$$

The scale law (12.53) can be written as

$$N(l) \propto l^{\kappa} \; . \tag{12.54}$$

The length of the Koch's curve is then with a scale length l

$$L(l) = l \cdot N(l) \propto l^{\kappa + 1} \; . \tag{12.55}$$

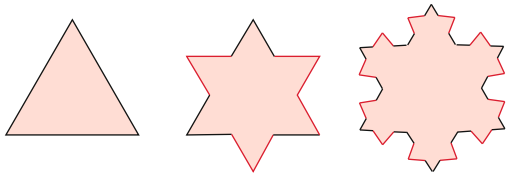

Figure 12.19 Koch's curve in closed form

This shows again that $\lim_{l\to 0} L(l) = \infty$, although the direct distance $\Delta = x_1 - x_2$ between the two ends (start point and endpoint) of the Koch's curve remains finite. The reason for the infinite length of the curve is the increasing refinement of the tooth structure.

Covering the curve by $N(l)$ squares with side length l, which are put together, the total area of all squares is

$$A(l) = l^2 \cdot N(l) \propto l^2 \cdot l^{\kappa} = l^{0.7382} .$$

The limit of this area is

$$\lim_{l\to 0}(A(l)) = 0 .$$

The Koch's curve is in a certain sense more than a one-dimensional line (because its length tends with $l \to 0$ towards infinity. It is, however, less than a two-dimensional area (because its area, defined by the squares, converges to zero).

If a fictional dimension is attribute to the Koch's curve it should be between 1 and 2.

One can formally define the d-dimensional volume, where d is an arbitrary number (not necessarily an integer)

$$V_d(l) \propto l^d \cdot N(l) \propto l^{d+\kappa} , \qquad (12.56)$$

the value of $\lim_{l\to 0}(V_d(l))$ jumps at $d = -\kappa$ from ∞ to 0.

The number

$$d = d_f = -\kappa \qquad (12.57)$$

is defined as the *fractional dimension* of the curve or area, because $d_f = 1.2618$ is not an integer but by the fraction 0.2618 larger the 1. For this value of d_f the d_f-dimensional volume V_{d_f} has a finite value, that is independent of the scale actor. From (12.47) it follows for $d = -\kappa$

$$V_{d_f}(\lambda \cdot l) \propto (\lambda \cdot l)^{d_f+\kappa} = (\lambda \cdot l)^0 = 1 . \qquad (12.58)$$

When the Koch's curve is drawn in a closed form (Fig. 12.19) one can see, that it surrounds a finite area, that remains finite even for $l \to 0$ although the length of the surrounding curve tends to infinity.

The fractional dimensions were already introduced by Felix Hausdorff (1868–1942). The fractional dimension d_f of the volume V_d which jumps from ∞ to 0 at $d_f = -\kappa$ is therefore also called the *Hausdorff dimension*.

There are many more examples for entities with fractional dimensions. One of them is the plane *Sierpinski lattice*, shown in Fig. 12.20. It is constructed by dividing the area of an equilateral triangle into four sub-triangles with equal areas and then remove the middle triangle. Its fractional dimension is

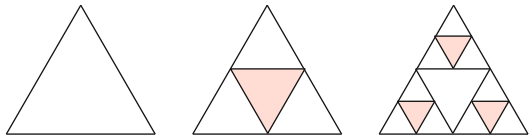

Figure 12.20 Construction of the Sierpinski-grid

$$d = \frac{\ln 3}{\ln 2} = 1.5849\ldots .$$

12.8 Mandelbrot Sets

In Sect. 12.2 we have illustrated for the example of the Verhulst dynamics the path from a stable system over the bifurcation point to the chaotic regime. A more general way to chaos, which leads to very beautiful computer graphics, was shown 1980 by B. Mandelbrot [12.9].

The basic idea relies on a nonlinear feedback algorithm for complex numbers. Instead of the one-dimensional iteration (12.26) of the logistic growth here points in the two-dimensional plane of complex numbers are used, following the iteration rule

$$z_{n+1} = z_n^2 + c , \qquad (12.59)$$

where c is a complex number, which determines the pattern of the generated points in the complex plane. For a given initial starting point z_0 the sequence z_n can be calculated by the computer according to the scheme in Fig. 12.21 and plotted in the x–y-plane.

We will illustrate this by some examples:

- $c = 0$, initial start value z_0 with $|z_0| < 1$. With increasing n the z_n decrease more and more and the points in the x–y-plane spiral towards $z_\infty = 0$ which is the attractor for all z-values with $|z| < 1$, i. e. for all points inside the circle with radius $r = 1$ (Fig. 12.22).
  For a starting value z with $|z| > 1$ the sequence z_n diverges. One may formally call $z = \infty$ as the attractor for all points with $|z| > 1$. For start values z_0 with $|z_0| = 1$ all points of the sequence remain on the circle, because $|z_n| = |z_0| = 1$, the circle represents the borderline between the intake areas of the two attractors $z(A_1) = 0$ and $z(A_2) = \infty$.

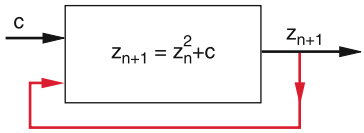

Figure 12.21 Iteration scheme for the generation of Mandelbrot sets

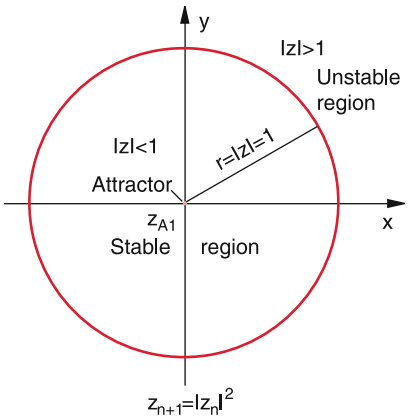

Figure 12.22 Stable range of the progression $z_{n+1} = z_n^2$ is the area inside the circle $|z| = 1$. All initial values with $|z_0| < 1$ converge against $z_\infty = 0$, with $|z_0| = 1$ against points on the circle and for $|z_0| > 1$ they diverge

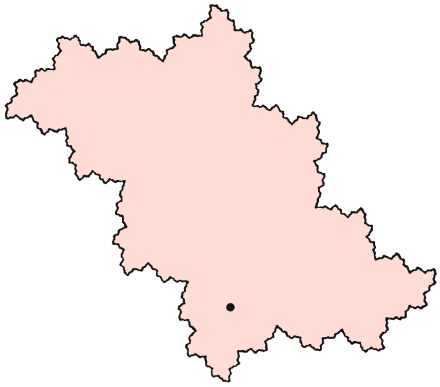

Figure 12.23 Boundary curve of the stable region for the parameter $c = -0.12375 + 0.56508\mathrm{i}$. The *black point* is the attractor

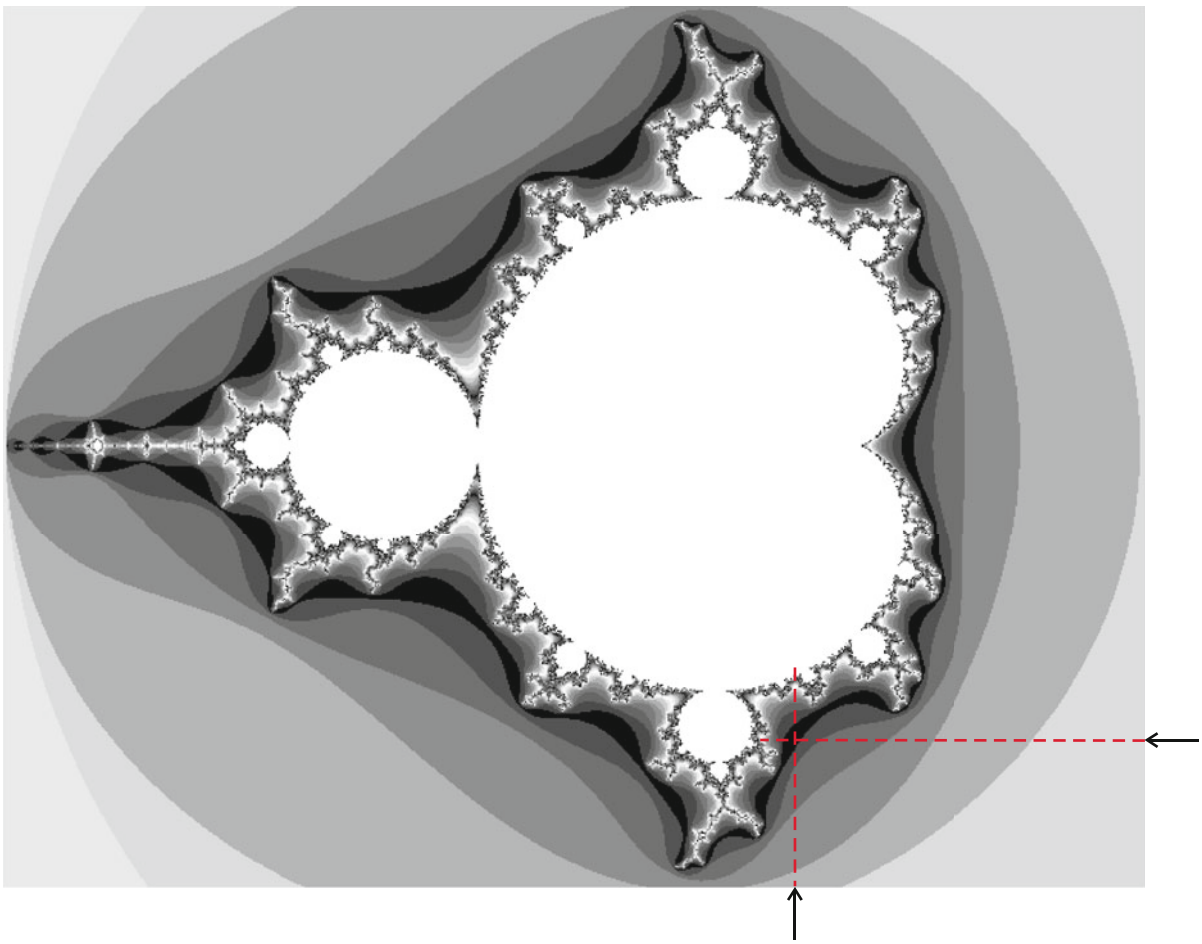

Figure 12.24 Mandelbrot set of all c-values for which the progression (12.59) with $z_0 = 0$ converges (*white area*). All *grey areas* represent c-values, that result in diverging progressions. The *shading* indicates the value of n at which z_n leaves the white area

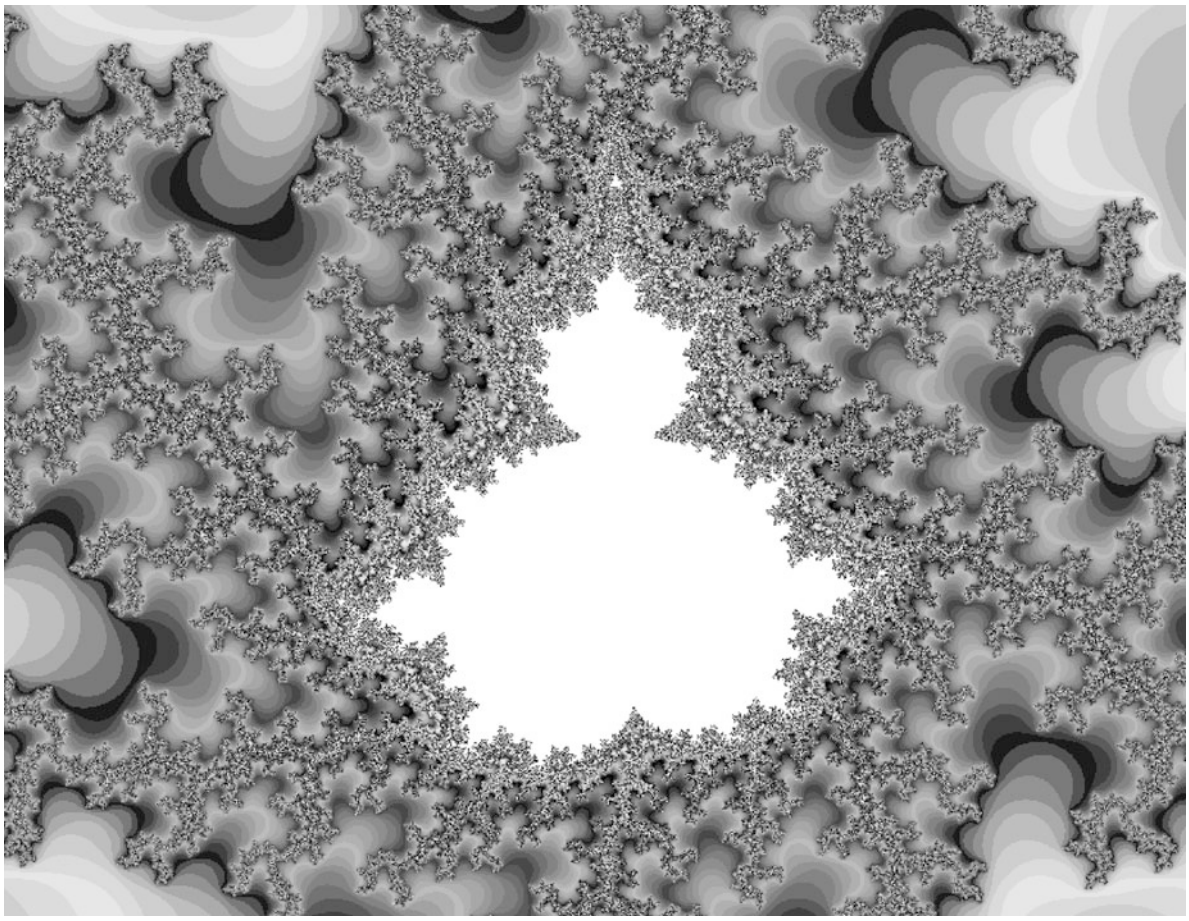

Figure 12.25 Strongly enlarged section of Fig. 12.24 around the intersection point of the two arrows, with an area of 1 mm^2 in Fig. 12.24

- If we choose $c \neq 0$ we get surprising sequences. For instance, starting with $z_0 = 0$ the sequence (12.59) reads:

$$z_1 = c\,; \qquad z_2 = c^2 + c\,;$$
$$z_3 = (c^2 + c)^2 + c\,; \quad \ldots\,.$$

For $c = 1 + \mathrm{i}$ this gives:

$$z_1 = 1 + \mathrm{i}\,; \quad z_2 = 1 + 3\mathrm{i}\,; \quad z_3 = -7 + 7\mathrm{i}\,;$$
$$z_4 = 1 - 97\mathrm{i}\,; \quad z_5 = -9407 - 193\mathrm{i}\,; \quad \ldots\,.$$

This shows that the points z_n in the x–y-plane perform large jumps from one to the next iteration step and that the sequence of our example diverges.

Also for $c \neq 0$ there is a region in the complex plane where the sequence converges. The attractor is now generally not zero and the borderline between stable and unstable regions is no longer a circle but (Fig. 12.23) a more complicated curve. Similar to the Koch's curve the borderline shows self-similarity i. e. it has a fractional structure. When it is magnified, every magnified segment shows a similar structure as the non-magnified larger section. Such self-similar border curves are called **Julia sets**.

The Mandelbrot set consists of all numbers c of the sequence (12.59) with $z_0 = 0$ that do not diverge. These are for instance all values of $c = a + \mathrm{i}b$ with $-2 < a < +1$ and $-1.5 < b < +1.5$. In order to generate the Mandelbrot set, one has to design a computer program that calculates for such sequences the border curves of the stable region.

Choosing, for instance, a rectangle $-A \leq x \leq +A$; $-B \leq y \leq +B$ in the complex plane, one can find out for every value of $c = x + \mathrm{i}y$ within this range, whether the sequence (12.59) converges or diverges. Now a certain colour is assigned to each value of c, depending on the number of iterations before the points c leave the rectangle. In Fig. 12.24 the colours are substituted by different grey shades. The white areas are the Mandelbrot set, imaging those z_n values which lead to stable sequences. Enlarging the tiny region in Fig. 12.24 which lies around the intersection of the two arrows, one gets the magnified Fig. 12.25.

The aesthetic beauty of such Mandelbrot sets becomes obvious with coloured computer graphics (see Fig. 12.26 and [12.10a–12.13]).

Figure 12.26 Coloured picture of the iteration $x \to \left((x^2 + q - 1)/(2x + q - 2)\right)^2$ with $\mathrm{Re}(q) = 1.2882–1.2963$ and $\mathrm{Im}(q) = 0.9695–0.9753$. The *large upper picture* is a magnified section of the central part in the *left lower picture* with different color choice. The *right lower picture* is the enlarged section, marked in the *lower left picture*, with $\mathrm{Re}(q) = 1.290681–1.291136$ and $\mathrm{Im}(q) = 0.97277–0.973098$ (With kind permission of Prof. H.O. Peitgen and Prof. P.H. Richter, Bremen)

12.9 Consequences for Our Comprehension of the Real World

Until the end of the 19th century most physicists were convinced, that all processes in nature proceed strictly deterministic and that it is, at least in principle, possible to determine the initial conditions of a system so accurately, that the future fate of the system can be exactly described for all times. This is substantiated by the famous statement of *Laplace*, published in 1776:

> The momentary state of a system is obviously the consequence of the state at an earlier moment. If we assume an intelligent creature that is able to calculate at one moment all relations between the different parts of the universe, it could predict all motions and all relations at all locations now and forever.

Such a **Laplace demon** would be able to predict the fate of all mankind if he knows the relevant data at a given time.

This strictly deterministic conception of the world arises the question: What can the free will of a human being change, if everything is already determined by initial conditions which we cannot influence? How much is a criminal responsible for his crime, if his future fate is already determined?

This strictly mechanistic conception has been shaken by two developments: The nonlinear dynamics and the quantum theory.

Poicaré, who has performed important spade work in nonlinear dynamics, wrote 1903:

> A very tiny effect, which we even may not notice, causes a large effect, that we cannot overlook. Then we say: This effect is accidental, because we have overlooked the real cause.

We see, that by no means the deterministic character of nature is questioned. This means that the principle of causality is accepted. However, the assumption that the initial conditions can be determined with sufficient accuracy, is no longer valid for instable systems, because here tiny changes of the initial conditions can cause large deviations of the final states. Often the uncertainty of the measurement limits the accuracy of predictions for many cases in nonlinear dynamics.

Quantum mechanics adds another principle argument: The uncertainty principle (see Vol. 3) states that it is impossible to determine exactly both the momentum and the position of a particle simultaneously. The more accurate one quantity is measured, the larger is the uncertainty for the other quantity. this implies that the initial state of a system cannot be determined with arbitrary accuracy, not only because of measurement errors, but because of the principle quantum mechanical restrictions.

For stable systems these small uncertainties have no big effect, but for unstable systems (chaotic systems) they can be disastrous, because they principally limit the predictions of future behaviour.

These few considerations illustrate that investigations of nonlinear phenomena bring about many new and surprising results when leaving the approximations of basic linear equations. This research field has developed only recently and more and more scientists are now interested in its basic physics and possible applications besides the gain of insight into the complexity of our real world [12.17–12.20].

There is in addition a psychological problem: How the spontaneous human interference in natural phenomena changes the predictability of processes and how spontaneous such interference really is, belongs into the field of psychology and cannot be solved in Physics.

Summary

- For phenomena described by nonlinear equations, the time development of the solutions often depends critically on the initial conditions. Unstable solutions are those, where infinitesimal small changes of the initial conditions cause large changes of the final states.
- The dynamical development of a system can be represented by a curve in phase space.
- The development of a system described by the Verhulst equation

$$x_{n+1} = a \cdot x_n - a \cdot x_n^2$$

  depends on the control parameter a. For certain values of a the solutions $x_f = \lim_{n\to\infty}(x_n)$ split into two possible values (bifurcation). For larger values of a each of these two values split again into two possible values. This splitting continuous with increasing a, until the chaotic regime is reached where no predictions of the final states are possible.
- Examples of applications of this equation are the population explosion, the parametric oscillator and the origin of traffic jams without identifiable causes, often caused by the delayed reaction of the driver.
- While for linear equations the superposition principle holds (i. e. with two independent solutions also their linear combination is a solution), this is no longer true for nonlinear equations. For special nonlinear equations the solutions show self-similarity.

- Self similarity is present, if

$$x(\lambda t) = \lambda^{\kappa} x(t) \Rightarrow x(t) t^{\kappa} \ ,$$

  where κ is a positive or negative number, not necessary an integer.
  The number κ is the fractional dimension.
- For self-similar solutions of nonlinear equations a natural scale is missing. An arbitrary stretching of time can be compensated by a corresponding change of the x-scale.
- All complex numbers which are generated by the sequence $z_{n+1} = z_n^2 + c$ form a set in the complex plane. The set of all non-divergent sequences with $z_0 = 0$ generate the Mandelbrot set.
- Such sets can be graphically displayed by simple computer programs.

Problems

12.1 A mass m is hold in its equilibrium position $(0, 0)$ in the x, y-plane by four springs with length L and restoring force constant k. aligned in the $\pm x$- and $\pm y$-directions.
a) What is the equation of motion, when the mass m is displaced in the $+x$-direction?
b) Bring this equation for $x \ll L$ in the form $\mathrm{d}^2x/\mathrm{d}t^2 + ax + bx^3 = 0$. How large are a and b?
c) What is the oscillation frequency for $bx^3 \ll a$ in the linear approximation and how does it change in the nonlinear form of the equation in b)?

12.2 Show, that the nonlinear equation in Probl. 12.1b with the initial conditions $x(0) = x_0$ and $\mathrm{d}x/\mathrm{d}t(0) = 0$ has periodical solutions.

12.3
a) Show that the non linear equation $m\,\mathrm{d}^2x/\mathrm{d}t^2 = -k_1x - k_2x$ with the initial conditions $x(0) = x_0$, $(\mathrm{d}x/\mathrm{d}t)(0) = 0$ can be transformed by the substitutions $\omega_0^2 = k_1/m$, $y = x/x_0$, $L^* = \omega_0 L$ into the dimensionless form $\mathrm{d}^2y/\mathrm{d}L^{*2} + y + \varepsilon y^2$ with $\varepsilon = x_0k_2/k_1$.
b) Calculate for $\varepsilon = 0.1$ the frequency shift against ω_0.

12.4 Determine the fix points for the system of differential equations $\mathrm{d}x_1/\mathrm{d}t = \lambda_1x_1 - \lambda_2x_1x_2$.
For which values of λ_1 and λ_2 are the fix points stable, metastable or unstable?

12.5 The equation of motion for the damped pendulum oscillation is $\ddot{\varphi} + \gamma\dot{\varphi} + \omega_0^2 \sin\varphi = 0$ with $\omega_0^2 = g/L$.
Determine the oscillation period $T(\varphi)$ and calculate the ratios $T(\varphi)/T(0)$ for $\varphi = \pi/4, \pi/2, (3/4)\,\pi$ and π.

12.6
a) What is the solution of the logistic growth function $\dot{z}(t) = az - bz^2$?
b) After which time has the function $z(t)$ doubled for $a = b$?
c) What is the limit for $z(t \to \infty)$?

12.7 Determine the fixpoints x_f and the Ljapunov exponent λ of the logistic equation $x_{n+1} = ax_n\,(1 - x_n)$ for $a = 3.1$ and $a = 3.3$.

12.8 Show, that the fractional dimension of the Sierpinski grid is $d_1 = 1.5849$.

12.9 Determine fixpoints and attractor for the differential equation in polar coordinates $\mathrm{d}r/\mathrm{d}t = -r\,(-a + r^2)$ for $a < 0$ and $a > 0$, $\mathrm{d}\varphi/\mathrm{d}t = \omega_0 = \text{const}$.

12.10 A particle with mass m moves in the potential $E_\mathrm{pot} = E_\mathrm{pot}(x_0) + a(x - x_0)^2 + b(x - x_0)^3$.
a) Determine the nonlinear equation of motion.
b) Up to which amplitude x_max is the solution a harmonic oscillation?

References

12.1a. J. Gleick, *Chaos: Making a New Science.* (Penguin Books, New York, 2008)
12.1b. E. Lorenz, *The Essence of Chaos.* (University of Washington Press, Washington, 1995)
12.2a. P. Bak, *How Nature works: The Science of Self-organizes Criticality.* (Copernicus Books, New York, 1996)
12.2b. St.A. Kaufman, *At Home in the Universe: The Search for the Laws of Self-Organization and Complexity.* (Oxford University Press, Oxford, 1996)
12.3. F.D. Peat, J. Briggs, *Timeless Wisdom from the Science of Change.* (Harper Collins Publ., New York, 1999)
12.4. T. Mullin, *The Nature of Chaos.* (Clarendon Press, Watton-under-Edge, UK, 1995)
12.5. P. Bergé, K. Pomeau, Ch. Vidal, *Order within Chaos.* (John Wiley, New York, 1984)
12.6a. G.L. Baker, J.P. Gollub, *Chaotic Dynamics.* (Cambridge University Press, Cambridge, 1996)
12.6b. M.J. Feigenbaum, J. Stat. Phys. **19**, 25–52 (1978)
12.7. W. Leutzbach, *Introduction in to the Theory of Traffic Flow.* (Springer, New York, 1987)
12.8. https://en.wikipedia.org/wiki/Self-similarity
12.9. B.B. Mandelbrot, *The Fractal Geometry of Nature.* (Freeman, San Francisco, 1982)
12.10a. H.-O. Peitgen, P.H. Richter, *The Beauty of Fractals.* (Springer, Berlin, Heidelberg, 1986)
12.10b. H.-O. Peitgen, *Chaos: Bausteine der Ordnung.* (Rowohlt, Hamburg, 1998)
12.11. See many articles in: *Chaos: An Interdisciplinary Journal of Nonlinear Science.* (American Institut of Physics)
12.12. H.J. Korsch, H.J. Jodl, *Chaos, A Program Collection for the PC.* (Springer, Berlin, Heidelberg, 1994)
12.13. H. Jürgens, H.O. Peitgen, D. Saupe (ed.), *Chaos and Fractals.* (Springer, Berlin, Heidelberg, 1993)
12.14. St.H. Strogatz, *Nonlinear Dynamics and Chaos: Applications to Physics, Biology, Chemistry and Engineering.* (Westview Press, Boulder, Colorado, USA, 2014)
12.15. G. Mayer-Kress (ed.), *Dimensions and Entropies in Chaotic Systems.* (Springer, Berlin, Heidelberg, 1986)
12.16. W.H. Steeb, A. Kunick, *Chaos und Quantenchaos in dynamischen Systemen,* 2nd ed. (Bibliographisches Institut, Mannheim, 1994)
12.17. B. Kaye, *Chaos and Complexity.* (VCH, Weinheim, 1993)
12.18. J. Parisi, St. Müller, W. Zimmermann (eds.), *A Perspective Look at Nonlinear Media.* (Springer, Berlin, Heidelberg, 1998)
12.19. L. Lam, *Nonlinear Physics for Beginners.* (World Scientific, Singapore, 1998)
12.20. R. Gilmore, M. Lefrane, *The Topology of Chaos.* (Wiley VCH, Weinheim, 2002)